© Indian Academy of Sciences

Electrical conductivity structure of Aravalli and Tural hot springs (western part of DVP) inferred from magnetotelluric data

P B V Subba Rao*[iD], Vasu Deshmukh, P V Vijaya Kumar
and A K Singh

Indian Institute of Geomagnetism, New Panvel, Navi Mumbai 410 218, India.
*Corresponding author. e-mail: subbarao.pbv@iigm.res.in

Both audio-magnetotelluric and magnetotelluric data were acquired across Aravalli and Tural hot springs (in Konkan region of Deccan volcanic province). The objective is to bring out the geoelectrical crustal structure beneath these geothermal zones. Two-dimensional inversion of data brings out different conductivity anomalies (i) shallow conductivity anomaly related to upward propagation of meteoric water through faults/fracture zones, (ii) major fracture/fault zones extending up to mid-crustal depths through which Deccan volcanism may have erupted and (iii) the presence of mid-crustal conductivity anomalies are related to trapped carbonate fluids that are linked to thermal effects of Deccan volcanism.

Keywords. Magnetotelluric; hot springs; Konkan region; Deccan volcanism; faults/fracture zones.

1. Introduction

Magnetotelluric (MT) studies are useful in bringing out subsurface structure in terms of electrical conductivity. Electrical conductivity is sensitive to conducting mineral phases (e.g., graphite, magnetite, etc.), fluid contents (filled free water or fluids released by dehydration mechanisms) and high heat flow (partial melting). In geothermal areas, resistivity variations are related to the presence of water (fluids), temperature and degree of mineralisation (Spichak and Manzella 2009). Hot subsurface water is closely related to structural fractured zones connected to medium–deep hot sources. The presence of fluids (especially hot water) and fractured zones are characterised by low resistivity. The resultant low-resistivity anomalies are the main target for the exploration of

geothermal zones by using MT methods (Simpson and Bahr 2005; Zhang *et al.* 2015). In India, MT/audio-magnetotelluric (AMT) investigations have been carried out across various geothermal zones: Puga valley geothermal field in NW Himalayas (Harinarayana *et al.* 2004, 2006; Abdul Azeez and Harinarayana 2007; Patro 2017), Chabsar hot water spring, Gujarat (Mohan *et al.* 2017) and Bakreswar geothermal province (Tripathi *et al.* 2019). These studies denote an anomalous conductivity zone (resistivity $\leq 10\,\Omega$m) at a shallow depth (≤ 2 km) related to the geothermal source in the region.

Aravalli, Tural and Rajawadi geothermal springs belong to the west coast geothermal province of India and occur at the foothills of the Western Ghats in Maharashtra. These springs are manifested as small pools along lineaments within the Konkan valley containing Deccan lava flows of

Cretaceous age (Monterio *et al.* 2019). Geother-mometry studies denote that the reservoir temperature of these hot springs is about 120 ± 10°C (Pitale *et al.* 1986; GSI 1991, 2002) and are characterised as low–medium enthalpy cate-gory based on surface hot water temperature (45–65°C) (Trupti *et al.* 2016). Geochemical stud-ies denote that thermal waters are alkali chloride (Cl–Na–Ca) type (Pitale *et al.* 1986; Sarolkar 2005; Chatterjee *et al.* 2016). Carbon dating of thermal waters for Tural spring is about 30 Ma and that of Rajawadi is about 17 Ma (Reddy *et al.* 2013) and these springs are recharged by meteoric waters through conduits (Pitale *et al.* 1986; Sarolkar 2005; Reddy *et al.* 2013; Ansari *et al.* 2014; Chat-terjee *et al.* 2016). Trace elements denote the cir-culation of meteoric water through the granitic basement (Sarolkar 2005; Reddy *et al.* 2013; Trupti *et al.* 2016).

Various geophysical studies have been carried out across Aravalli, Tural and Rajawadi geother-mal zones are micro-gravity, micro-magnetic (Low *et al.* 2020) and DC resistivity sounding (Kumar *et al.* 2011). Analysis of gravity and magnetic data brings out vertical to sub-vertical conduits system extending to a geothermal source and a shallow granite–gneiss basement. Electrical resistivity tomography across Aravalli, Tural and Rajawadi hot springs brings out a low-resistivity zone in the depth range of 50–200 m associated with source region of geothermal spring (Kumar *et al.* 2011). As these studies are limited to shallow subsurface, we have carried out detailed AMT/MT studies to determine the subsurface structure of these geothermal zones in terms of electrical conductiv-ity distribution.

2. Geology and tectonics

West coast fault (WCF) is a major tectonic feature in Deccan volcanic province (DVP) along which the thermal springs are present (Chandrasekharam 1985). Several authors believe that WCF has formed in two stages: (i) the initial northern frac-turing is associated with the early rifting episode between India and Madagascar at ∼84 Ma (Owen 1976; Biswas 1982; Storey *et al.* 1995; Bhat-tacharya and Yatheesh 2015). (ii) The later extension of the fracture towards the south is associated with the rifting stage between India and Seychelles (Owen 1976; Gombos *et al.* 1995; Mukherjee *et al.* 2017).

Different lava flows identified in Deccan trap region are (i) compound pahoehoe flows (Pitale *et al.* 1986; Bondre *et al.* 2004), (ii) simple flows consisting of slabby pahoehoe (Duraiswami *et al.* 2003), (iii) rubbly pahoehoe (Duraiswami *et al.* 2008) and (iv) aa flows (Brown *et al.* 2011; Dur-aiswami *et al.* 2014). Most of the lava flows in Tural–Rajwadi group of hot springs area are of sheet pahoehoe and rubbly pahoehoe types similar to those exposed in the adjacent Koyna region (Duraiswami *et al.* 2017).

Most of the lineaments on the west coast are in the direction of the NNW–SSE being parallel to the Western Ghats (Arora *et al.* 2018) as shown in figure 1. Similarly, NS trending gravity high with steep gradients are located along the western margin (Kailasam *et al.* 1972) and indicates the presence of the secondary magma chamber (Negi *et al.* 1992) or underplating magmatic material (Radhakrishna *et al.* 2002) during the Deccan volcanism. Deep Seismic Sounding (DSS) studies (Kaila *et al.* 1981) denote that thickness of the crust decreases as one move from Western Ghats (∼40 km) to west coast (30 km) and increase in trap thickness from 0.6 to 1.5 km. Similar results were obtained by Dev *et al.* (2012) based on gravity studies. Micro-earthquake studies in western part of India (within DVP) have been attributed to reactivation of the basement faults (Chadha 1992; Mohan *et al.* 2007). Most of the geothermal zones occurring along the west coast have been related to the erosion of traps (release of stress) facilitating
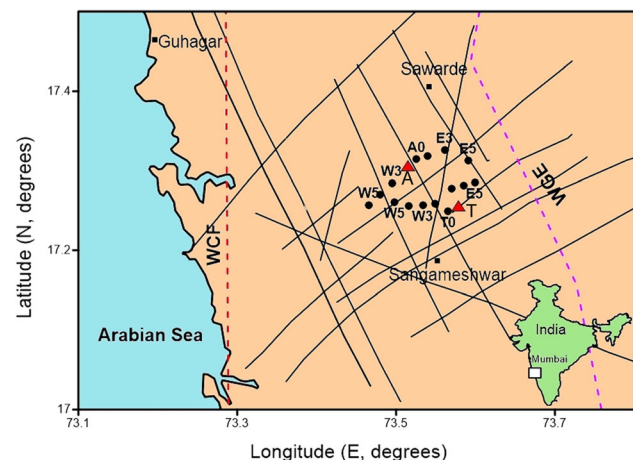

Figure 1. Hot springs of Aravalli (A) and Tural (T) located in the western part of Maharashtra along with AMT/MT sites are shown. Regional lineaments of the study area (after Arora *et al.* 2018) are superimposed. It also shows WCF, WGE and geothermal zones (A and T) that are located to the west of WGE.

upwelling of deep fluids (Raval and Veeraswamy 2003). Aravalli, Tural, Rajawadi and Rajpur hot springs occur in Konkan region and are youngest springs that overlie the basement rocks (Trupti *et al.* 2016). One of the major lineaments present towards north of the study area is Panvel flexure (Auden 1949; Dessai and Bertrand 1995; Sheth 1998) and its origin is related to west coast rifting, subsidence and the uplift of the Western Ghats (Devey and Lightfoot 1986; Watts and Cox 1989). The Western Ghats escarpment (WGE) is thought to be a rift-bounding fault of the west coast passive margin (Gunnell and Fleitout 1998; Kale 2010). WCF and WGE are shown in figure 1.

3. MT data and analysis

3.1 *MT data*

In MT, the subsurface electrical conductivity is obtained by using the natural electromagnetic fields as a source in the frequency range 10^{-5}–10^5 Hz. Both MT and AMT surveys were carried out along two profiles (across Aravalli and Tural hot springs) with station spacing of about 1 km having a profile length of about 8–10 km. In the current study, AMT data were acquired in the period range 10^{-4} to 1 s by using MTU-5A instruments (Phoenix, Canada). Similarly, broad-band MT data were acquired in the period range of 0.0025–1000 s. Both data sets are processed by using SSTM 2000 processing software which works on the principle of robust cascade decimation technique to improve the signal-to-noise ratio (Jones and Jodicke 1984; Jones *et al.* 1989). AMT is useful for mapping shallow structures, while MT data are used for mapping crust–lithosphere structures. Thus, both data sets were combined by using winglink software and period range available for modelling and interpretation is from 10^{-4} to 10^2 s that is presented as apparent resistivity and phase curves as shown in figure 2(a and b).

As seen in figure 2(a), apparent resistivity curves denote that the eastern part of the Aravalli profile is more resistive than the western part. Station APA0 located near Aravalli hot spring has characteristics similar to the eastern part of the profile. Figure 2(b) brings out the nature of the Tural profile suggesting that the eastern part is more resistive than the western part. Station TPT0 is located over Tural hot spring and low resistivity is observed at shorter periods.

3.2 *Dimensionality analysis*

Prior to MT data modelling, it is essential to understand the dimensionality of the data for obtaining the subsurface dimension as well as the direction of the underlying structures. In the current study, the dimensionality analysis has been performed by using Bahr (1991) skew and phase tensor analysis (Caldwell *et al.* 2004).

3.2.1 *Bahr skew*

Skewness is the first parameter used in MT for determining the dimension of subsurface structures. In the current study, we have estimated Bahr skew for both the profiles that depend upon the phases of the impedance tensor and are defined by

$$\text{Bahr's skew} = \frac{|[D_1 S_2] - [S_1 D_2]|^{1/2}}{|D_2|},$$

where $S_1 = Z_{xx} + Z_{yy}$, $S_2 = Z_{xy} + Z_{yx}$, $D_1 = Z_{xx} - Z_{yy}$ and $D_2 = Z_{xy} - Z_{yx}$.

Generally, if skew values are greater than 0.3 then it implies that the MT data are three-dimensional (3D). Bahr skew values calculated for both the profiles are shown in figure 3(a and b). As observed in figure 3(a), skew values are varying from 0 to 0.3 for Aravalli stations except at the periphery station APW3 (denoting 3D nature at shallow depth) indicating that the structure is one-dimensional/two-dimensional (1D/2D) in nature. Similarly in figure 3(b), skew values vary from 0 to 0.3 denoting 1D/2D nature for Tural stations except at stations TPW2 and TPT0 that show 3D nature at higher periods.

3.2.2 *Phase tensor analysis*

The other method used to infer the dimensionality is phase tensor. Caldwell *et al.* (2004) have defined a phase tensor $\phi = XY^{-1}$, where X and Y are real and imaginary components of the impedance tensor which are unaffected by galvanic distortions in the observed MT data. Therefore, rotation of the tensor to get the coordinate invariant principal components ($\phi_{\min}$, $\phi_{\max}$) gives the strike direction with the 90° ambiguity. The phase tensor approach does not invoke any assumption about the dimensionality of the regional conductivity structure that enables the robust estimates of distortion parameters and regional strike.
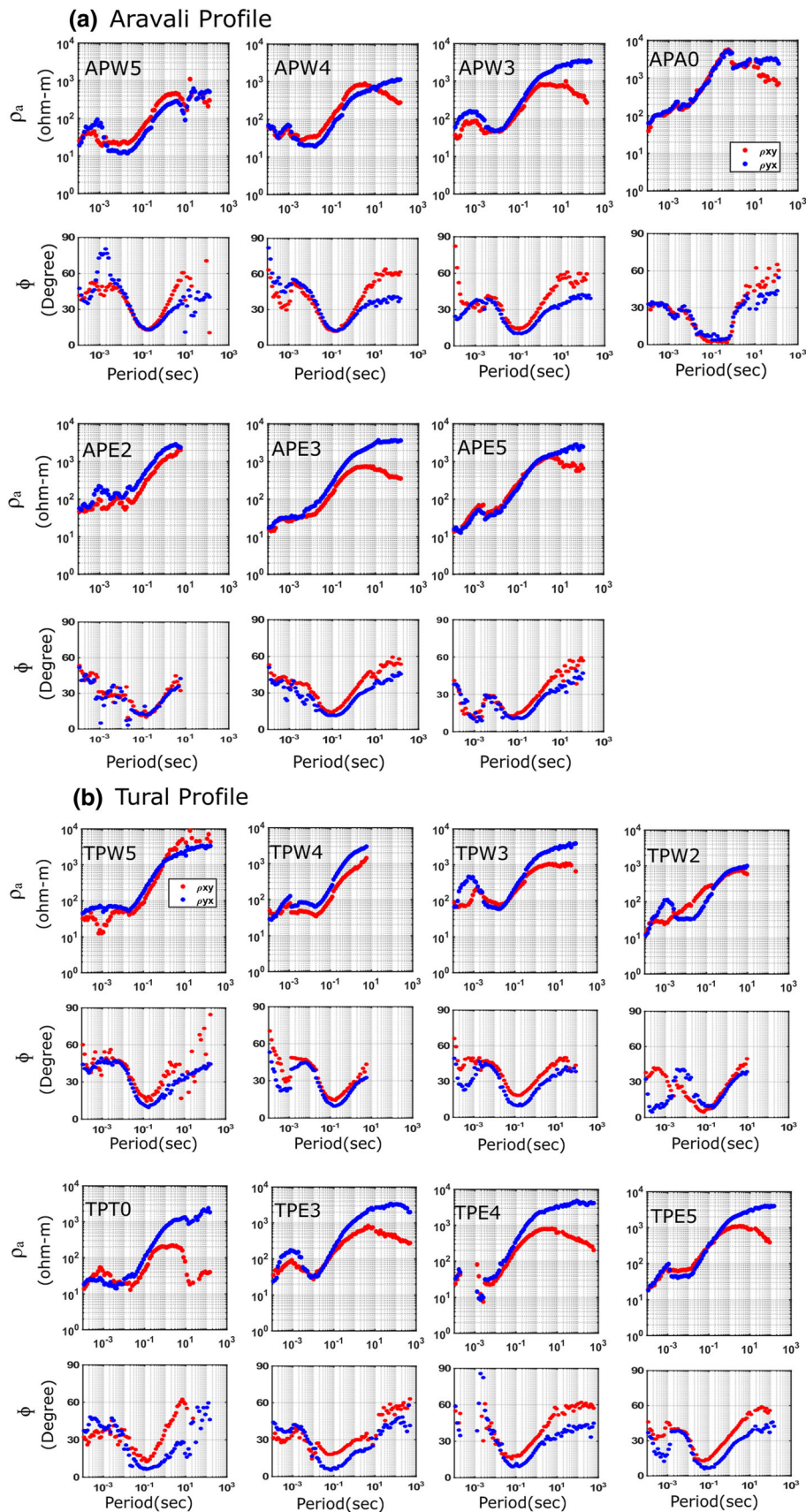
(a) Aravali Profile

Figure 2. Observed apparent and phase curves across (**a**) Aravalli hot springs and (**b**) Tural hot springs. These curves denote that eastern part of the profile is resistive than the western part.
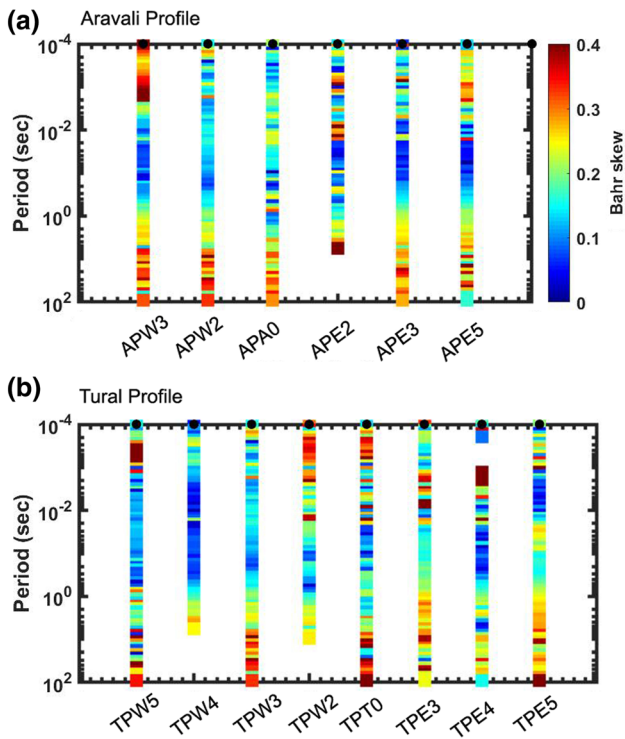
Figure 3. Dimensionality parameters: Bahr's skew for both (**a**) Aravalli and (**b**) Tural profiles denoting 2D nature of the data.

The phase tensor is represented by an ellipse that is defined by (i) the maximum phase (Φ_{max}), (ii) the minimum phase (Φ_{min}) and (iii) the skew angle (β). The Φ_{max} and Φ_{min} define the major and minor axes of the ellipse and are equal if it is 1D structure (ellipse becomes a circle). The skew angle (β) provides a measure of the dimensionality of the MT data and falls in the range of ±5 if the subsurface structure is 1D or 2D. The phase tensor ellipses of all stations are shown in figure 4. At small periods (between 0.1 and 1 s), ellipses are becoming circles and skew angle is less than ±3°, which denote the 1D and 2D nature of the data. Above 1 s, the skew value is in the range of ±5° denoting 2D nature of the MT data. The direction of the phase tensor ellipses is aligned along NE–SW suggesting regional strike direction (plotted on Python platform after Krieger and Peacock 2014) that correlates very well with the strike direction obtained from Groom–Bailey (GB) analysis.

3.3 *Geo-electrical strike*

GB method is often used in tensor decomposition of MT impedance and is based on solving a system of nonlinear over-determined equations composed of regional impedance tensor and distortion equations (Groom and Bailey 1989, 1991; Jones 2012). In the current study, we have carried out geoelectrical strike analysis (McNeice and Jones 2001) that estimates distortion and geometrical parameters from the data by assuming a regional electric 2D subsurface with 3D superficial distortion.

In the current study, regional strike assessed through GB technique suggests an N60°E direction as shown in figure 5. In 2D analysis and interpretation process, the impedance tensor at each station was rotated by N60°E. Thus, rotation of the impedance tensor allows for decoupling into the transverse electric (TE) and transverse magnetic (TM) modes.

4. 2D modelling of MT data

In the current study, electrical conductivity models were derived from Tural and Aravalli (AMT plus MT) data by using the algorithm of Rodi and Mackie (2001), as implemented in the Winglink software package. 2D inversion for two profiles were carried out by using uniform $100\,\Omega\,m$ half-spaces as starting models. An appropriate value of the regularisation parameter(s) needed to achieve a trade-off between the root-mean-square (RMS) error of misfit and the smoothness of the model. A regularisation trade-off curve (Hansen 1992), which is optimally L-shaped, was used to obtain the most appropriate smoothing operator τ for each set of inversions. Trade of curves were obtained for each value of τ, gradually increasing τ from 1 to 100, running 2D inversion for each value of τ, and plotting resultant RMS errors *vs.* τ values. After observing L-curves (as shown in figure 6), a τ value of 5 was selected for inversion of Aravalli and Tural data. Booker *et al.* (2004) recommended that error floors in the impedance tensors can be improved until a distortion model fitted the data with a satisfactory misfit. After trying different combinations of error floors, error floors for apparent resistivity and phase were set to be 20% and 5% for both TE and TM modes. Interpreted models show a shallow conductivity anomaly related to hot springs and a conductivity zone (deep-seated fractured/fault zone) sandwiched in between resistivity blocks as shown in figures 7 and 8. Comparisons between observed and calculated pseudo-sections are shown in figure 9.
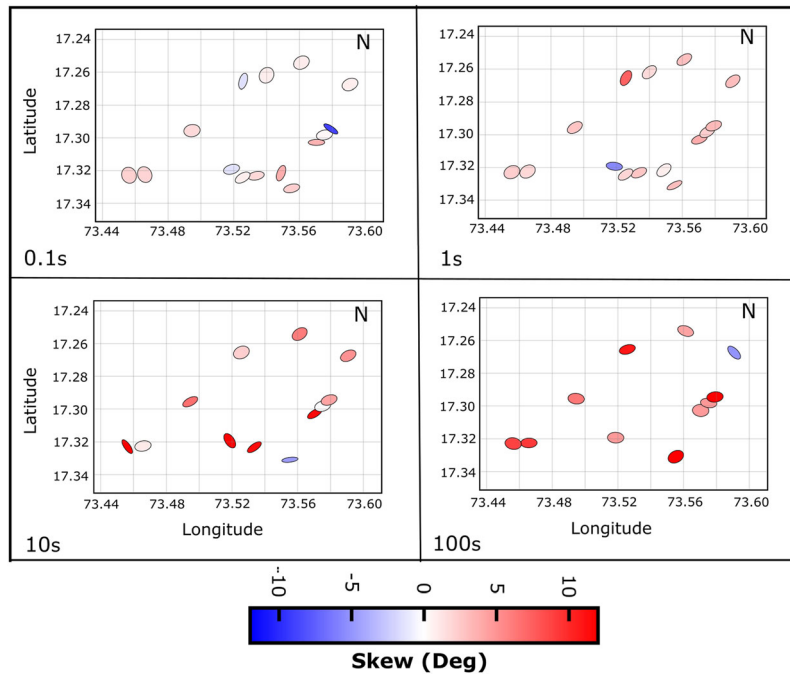
Figure 4. Phase tensor ellipses for both Aravalli and Tural profiles for 0.1–100 s. Major axes of the ellipses are oriented in NE–SW direction with $|\beta| \leq \pm 5$ suggesting 2D in nature.
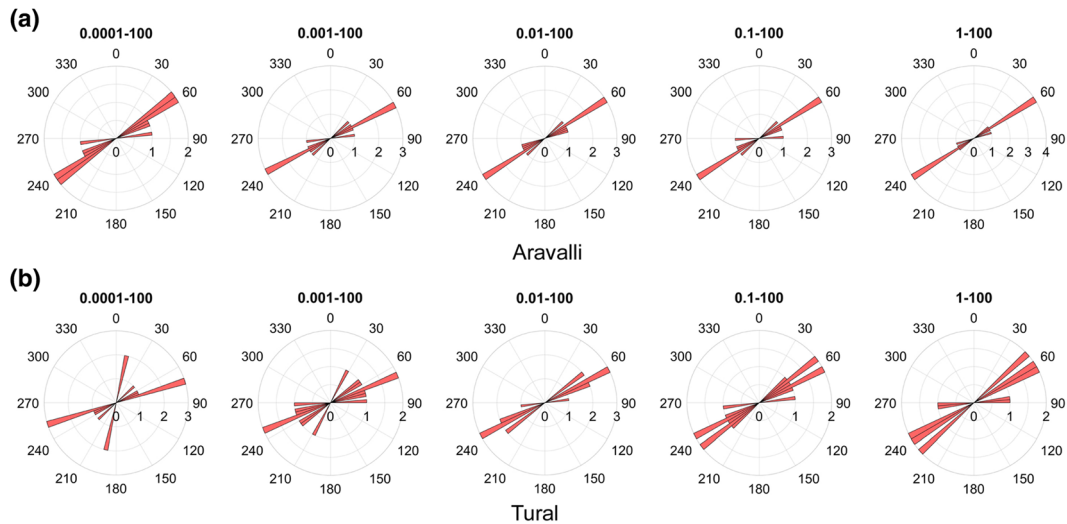

Figure 5. Multi-frequency Rose diagram of two west–east profiles showing geoelectrical strike direction by using GB (Groom and Bailey 1989) tensor decomposition technique. Regional strike obtained is about N60°E along (**a**) Aravalli and (**b**) Tural hot spring zones.

4.1 *Sensitivity analysis*

Before making any interpretations, sensitivity analysis is carried out for the model resolution because the resistivity of the starting model used for the inversion is a homogeneous half-space with a value of 100 Ω m. We have carried out the sensitivity analysis by masking conductivity anomaly C1 obtained in Aravalli profile with a resistivity value of surrounding

formations (test model as shown in figure 10b) and then restarted forward modelling. Comparison of RMS value of forward modelling (22.1) with inversion model (1.35, figure 10c) suggests that the conductive feature is required by MT data.

Similar test is carried out for Tural profile (as shown in figure 11a and b) by replacing mid-lower crustal conductivity anomaly (C2) with the resistivity value of the surrounding rocks (figure 11b).
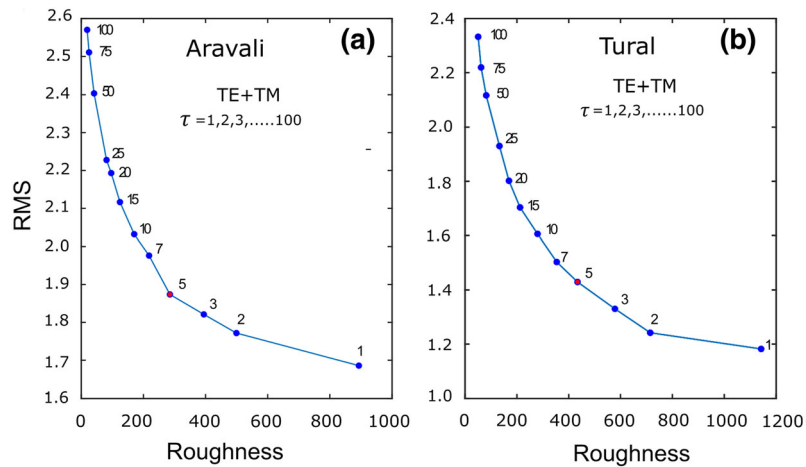
Figure 6. L-curves obtained for (**a**) Aravalli and (**b**) Tural profiles for estimating regularisation parameter τ during 2D inversion.
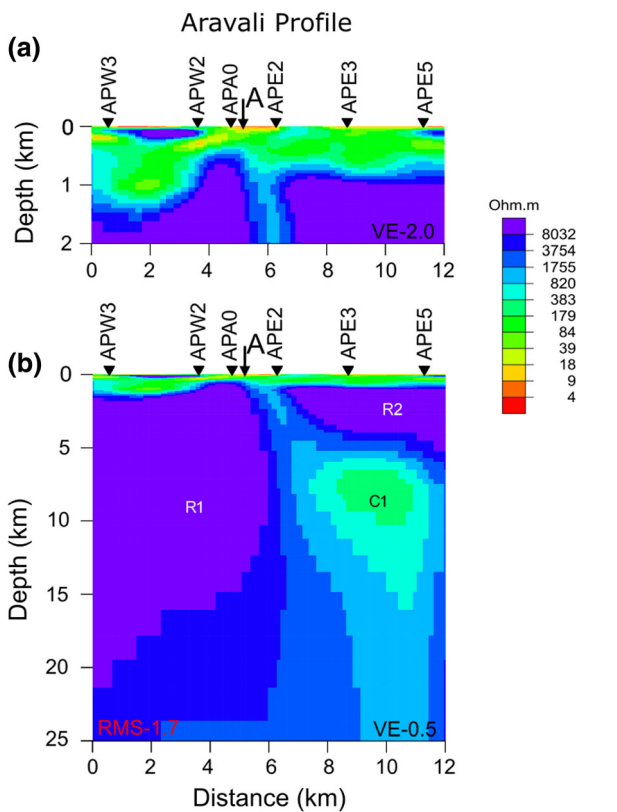

Figure 7. 2D geoelectric depth section (TE + TM mode) across Aravalli profile. (**a**) Shallow section showing high conductivity anomaly beneath Aravalli hot spring. (**b**) Deep-seated conductivity fault/fracture zone along with trapped carbonate fluids (C1) at brittle–ductile zone.

Both forward and inversion modelling is carried out. The modified model shown in figure 11(c) suggests the presence of the conductive model. Thus, the conductive features (as shown in model figures 10c and 11c) are required to explain the observed TE and TM mode data sets.
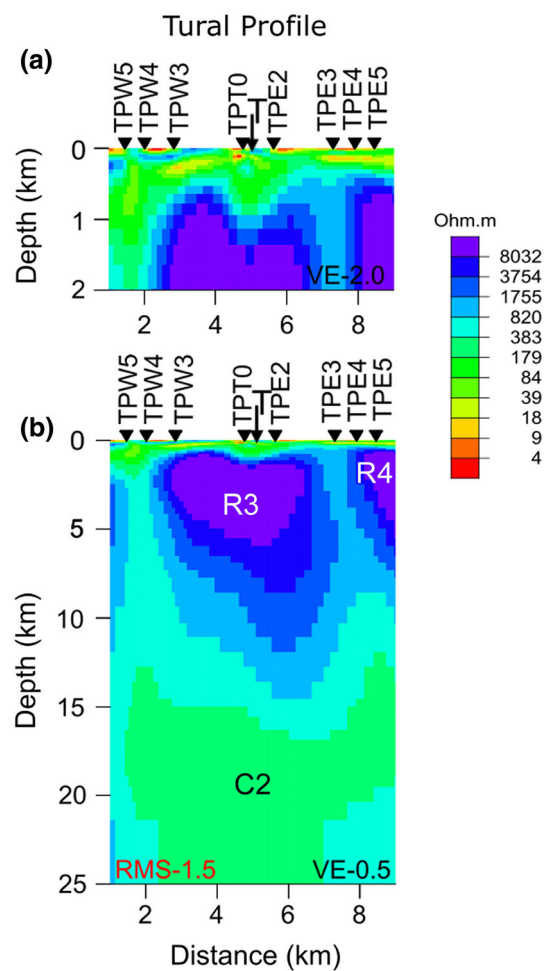
Figure 8. Geoelectric structure beneath Tural hot spring that is reflected as a high conductivity anomaly at shallow depth (**a**) along with an intrusive body (S) at shallow level below station TPT0 and acts as a source rock. Deeper section, (**b**) showing two different fault/fracture zones along with Deccan volcanism has spread both horizontally and vertically. Mid–lower crustal conductivity anomaly (C2) related to accumulation of basaltic magma at the base of the crust.
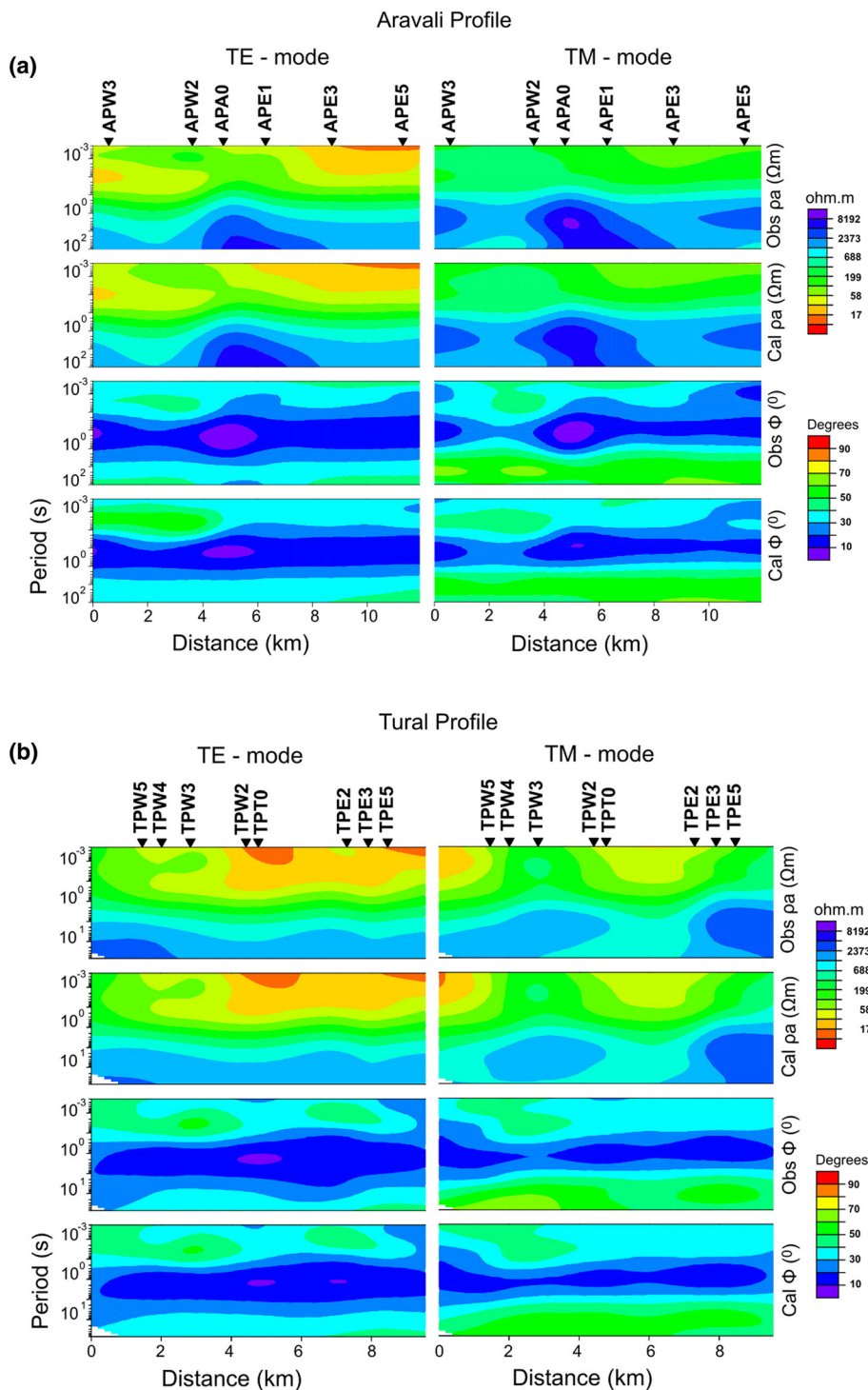
Figure 9. Pseudo-sections for observed and computed TE and TM mode data along (**a**) Aravalli profile and (**b**) Tural profile.

5. Results and discussion

The 2D geoelectric section along geothermal profiles (figures 7 and 8) brings out conductive (C1 and C2) and resistive zones (R1, R2, R3 and R4) in the upper and the mid-crustal levels suggesting a strong heterogeneous electrical resistivity structure. In the current study, 2D models obtained for shallow (3 km)

and deeper sections (up to 25 km) for Aravalli and Tural geothermal regions are discussed below.

5.1 *Shallow section*

In the current study, the thickness of the Deccan basalts increases as one moves from east (800 m) to west (∼1.5 km) and its resistivity varies from 50 to
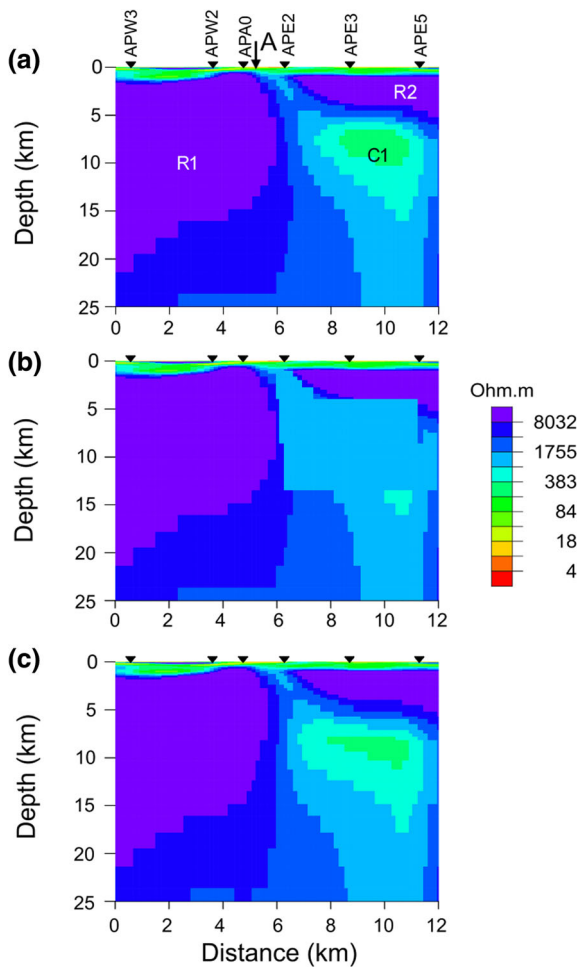
Figure 10. Sensitivity analysis is carried out for Aravalli profile. (**a**) The original inversion model is modified by masking the conductor (C1) with surrounding resistivity values as shown in (**b**). The second inversion also brings out the original model as shown in (c).

Figure 11. Sensitivity analysis is carried out for Tural profile. In the original model (**a**), mid–lower crustal conductivity anomaly (C2) is masked by the resistivity values of surrounding rocks (**b**). Reinversion brings out original model as shown in (**c**).

$200 \, \Omega \, \mathrm{m}$. Different lava flows have been deposited in low-lying Konkan region as suggested by Duraiswami *et al.* (2014) and is related to the development of WGE (Radhakrishna *et al.* 2019).

In these low-temperature geothermal activities, fluids are driven by Western Ghats, which circulate to a depth of 1–2 km (basement depth obtained from AMT studies) in the crust where they are heated by the geothermal gradient. The circulation of meteoric water through the granitic basement is denoted by the trace-element characteristics (Reddy *et al.* 2013). These fluids gushed up to the surface through faults/fractures and reflected as hot springs. These are observed as shallow conductivity anomalies beneath Aravalli station (APA0) and Tural station (TPT0). The age of Tural spring is about 3080 years BP (Reddy *et al.* 2013) and suggests long-term circulation of meteoric waters. It is further supported by the presence of total quantity of He in the associated gas
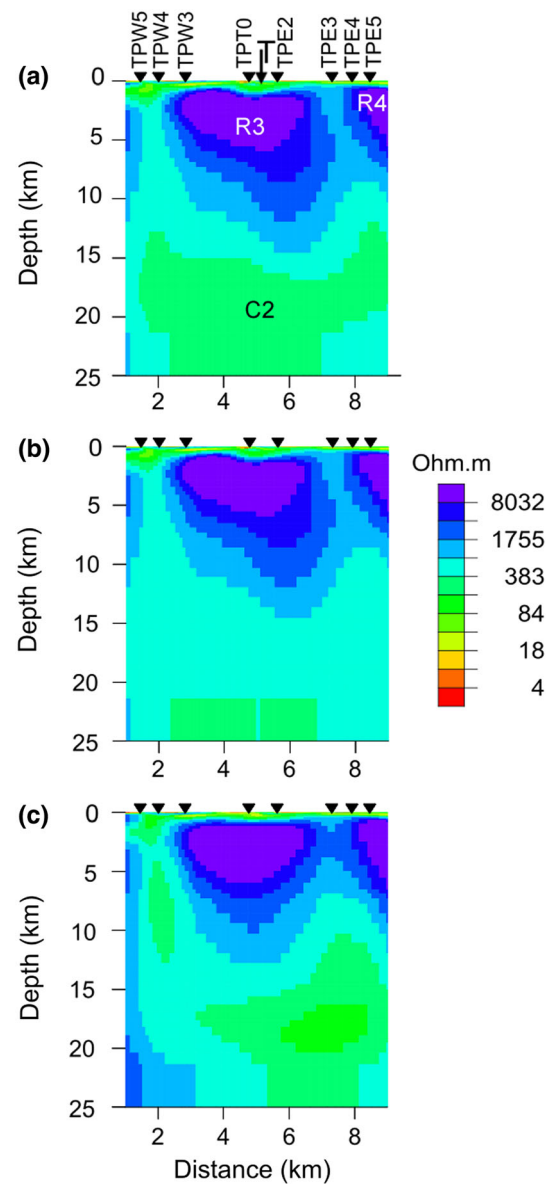
phase (Minissale *et al.* 2000). It is also noticed that surface hot water temperature at Tural is greater than Aravalli (Reddy *et al.* 2013) and possible could be related to the presence of the source rock (S) at shallow depth beneath Tural hot spring. This source rock could be a volcanic plug over which meteoric water circulates.

5.2 *Deeper section*

MT studies across Aravalli and Tural hot springs bring out a deep-seated fracture/fault zones (F1 (in

between R1 and R2), F2 (western part of R3) and F3 (eastern part of R3)) extending to the upper crustal depths ($\sim$10–15 km) and may have facilitated Deccan magma spreading both vertically as well as horizontally. These linear conductivity zones may be related to the source of fluids at the fracture/fault zones at mid-crustal depths due to dehydration of minerals during metamorphism (Byerlee 1993). An upward movement of deeper fluid and/or mineral solutions would trigger hydrofracturing and establish an intermittent hydraulic connectivity between near-surface and deeper fluid systems (Raval 1993) through fault/fracture zones (F1, F2 and F3).

Intermediate crustal conductivity anomalies, C1 is observed beneath Aravalli hot spring and C2 beneath Tural hot spring. The possible causes for these conductivity anomalies can be explained in terms of fluids/volatiles (CO_2 and H_2O) that have been released in the deep crust along the western margin of India due to thermal effects associated with the Deccan volcanism (Raval 1995; Sen 2001). These fluids are expelled due to compression (Muir-wood and King 1993) and metamorphism (Sandiford and Powell 1986; Nover 2005). They are trapped at intermediate crustal depths as described by Bailey (1994) forming brittle–ductile zones. Thus, conductivity zones C1 and C2 may represent trapped fluid zones related to brittle–ductile transition zones.

Resistivity blocks (R1, R2, R3 and R4) may represent the modified Precambrian crust after Deccan volcanism. The inference that the crust underlying the DVP is Precambrian type is brought out by seismic tomography studies (Chopra *et al.* 2014; Praveen Kumar and Mohan 2014), geochemical studies (Ray *et al.* 2008) and deep drilling project in Konya region (Gupta *et al.* 2017). Later, mafic/ultramafic intrusions due to Deccan volcanism and recrystallisation of blocks may have given rise to high resistive values. Geological evidence of mafic intrusions in Panvel flexure and surrounding regions has been identified by Dessai *et al.* (1990).

6. Conclusions

Integrated AMT and MT studies across hot springs (Aravalli and Tural) bring out two different conductivity anomalies: (i) shallow anomaly is related to upward propagation of meteoric water through faults/fracture zones (hot springs) and (ii) mid–lower crustal conductivity anomalies (C1 and C2) are related to carbonate fluids released/trapped due to thermal effects associated with Deccan volcanism.

Author statement

PBV Subba Rao, Vasu Desmukh and PV Vijaya Kumar have made substantial contributions towards the conceptualization and acquisition of AMT/MT data along the Aravalli and Tural geothermal regions as well as for analysis and interpretation of data. Subba Rao and Vasu have been involved in drafting the manuscript and its interpretation. AK Singh: Reviewing and editing.

References

Abdul Azeez K K and Harinarayana T 2007 Magnetotelluric evidence of potential geothermal resource in Puga, Ladakh, NW Himalaya; *Curr. Sci.* **93** 323–330.

Ansari M A, Sharma S, Kumar U S, Chatterjee S, Pant D and Low U 2014 Hydrogeological controls of radon in a few hot springs in the Western Ghats at Ratnagiri district in Maharashtra, India; *Curr. Sci.* **107** 1587–1590.

Arora K, Srinu Y, Gopinadh D, Chadha R K, Raza H, Mikhailov V, Ponomarev A, Kiseleva E and Smirnov V 2018 Lineaments in Deccan basalts: The basement connection in the Koyna–Warna RTS region; *Bull. Seismol. Soc. Am.* **108** 2919–2932.

Auden J B 1949 Dykes in western India: A study of their relationships with the Deccan Traps; *Trans. Natl. Inst. Sci. India* **3** 123–157.

Bahr K 1991 Geological noise in magnetotelluric data: A classification of distortion types; *Phys. Earth Planet. Int.* **66** 24–38.

Bailey M C 1994 Fluid trapping in mid-crustal reservoirs by H_2O–CO_2 mixtures; *Nature* **371** 238–240.

Bhattacharya G C and Yatheesh V 2015 Plate-tectonic evolution of the deep ocean basins adjoining the western continental margin of India – A proposed model for the early opening scenario; In: *Petroleum geosciences: Indian contexts* (ed.) Mukherjee S, Springer Geology, https://doi.org/10.1007/978-3-319-03119-4_1.

Biswas S K 1982 Rift basins in western margin of India and their hydrocarbon prospects with special reference to Kutch basin; *Bull. Amer. Assoc. Pet. Geol.* **66** 1497–1513.

Bondre N R, Duraiswami R A and Dole G 2004 Morphology and emplacement of flows from the Deccan volcanic province, India; *Bull. Volcanol.* **66** 29–45.

Booker J R, Favetto A and Pomposiello M C 2004 Low electrical resistivity associated with plunging of the Nazca Cat slab beneath Argentina; *Nature* **429** 399–403.

Brown R J, Blake S, Bondre N R, Phadnis V M and Self S 2011 ´A´ ā lava flows in the Deccan volcanic province, India, and their significance for the nature of continental flood basalt eruptions; *Bull. Volcanol.* **73** 737–752.

Byerlee J 1993 Model for episodic flow of high-pressure water in fault zones before earthquakes; *Geology* **21** 303–306.

Caldwell T G, Bibby H M and Brown C 2004 The magnetotelluric phase tensor; *Geophys. J. Int.* **158** 457–469.

Chadha R K 1992 Geological contacts, thermal springs and earthquakes in peninsular India; *Tectonophys.* **213** 367–374.

Chandrasekharam D 1985 Structure and evolution of the western continental margin of India deduced from gravity, seismic, geomagnetic and geochronological studies; *Phys. Earth Planet. Inter.* **41** 186–198.

Chatterjee S, Sharma S, Ansari M A, Deodhar A S, Low U, Sinha U K and Dash A 2016 Characterization of subsurface processes estimation of reservoir temperature in Tural Rajwadi geothermal fields, Maharashtra, India; *Geothermics* **59** 77–89.

Chopra S, Chang T M, Saikia S, Yadav R B S, Choudhury P and Roy K S 2014 Crustal structure of the Gujarat region, India: New constraints from the analysis of teleseismic receiver functions; *J. Asian Earth Sci.* **96** 237–254.

Dessai A G and Bertrand H 1995 The 'Panvel flexure' along the western Indian continental margin: An extensional fault structure related to Deccan magmatism; *Tectonophys.* **241** 165–178.

Dessai A G, Rock N M S, Griffin B J and Gupta D 1990 Mineralogy and petrology of xenoliths-bearing alkaline dykes associated with Deccan magmatism, south of Bombay, India; *Eur. J. Mineral.* **2** 667–685.

Dev S V, Radhakrishna M, Chand S and Subrahmanyam C 2012 Gravity anomalies, crustal structure and rift tectonics at the Konkan and Kerala basins, western continental margin of India; *J. Earth Syst. Sci.* **121** 813–822.

Devey C W and Lightfoot P C 1986 Volcanological and tectonic control of stratigraphy and structure in the western Deccan traps; *Bull. Volcanol.* **48** 195–207.

Duraiswami R A, Bondre N R and Managave S 2008 Morphology of rubbly pahoehoe (simple) flows from the Deccan volcanic province: Implications for style of emplacement; *J. Volcanol. Geotherm. Res.* **177** 822–836.

Duraiswami R A, Dole G and Bondre N 2003 Slabby pahoehoe from the western Deccan volcanic province: Evidence for incipient pahoehoe-aa transitions; *J. Volcanol. Geotherm. Res.* **121** 195–217.

Duraiswami R A, Gadpallu P, Maskare B, Purwant A, Meena P, Krishnamurthy P and Mahabaleshwar B 2017 Volcanology and lava flow morpho-types from the Koyna–Warna region, western Deccan traps, India; *J. Geol. Soc. India* **90** 742–747.

Duraiswami R A, Gadpallu P, Shaikh T N and Cardin N 2014 Pahoehoe–a′a transitions in the lava flow fields of the western Deccan traps, India – Implications for emplacement dynamics, flood basalt architecture and volcanic stratigraphy; *J. Asian Earth Sci.* **84** 146–166.

Gombos A M, Powell W G and Norton I O 1995 The tectonic evolution of western India and its impact on hydrocarbon occurrences: An overview; *Sedim. Geol.* **96** 119–129.

Groom R W and Bailey R C 1989 Decomposition of magnetotelluric impedance tensors in the presence of local three-dimensional galvanic distortion; *J. Geophys. Res.* **94** 1913–1925.

Groom R W and Bailey R C 1991 Analytical investigations of the effects of near surface three dimensional galvanic scatterers on MT tensor decomposition; *Geophysics* **56** 496–518.

GSI 1991 Geothermal atlas of India; *Geol. Surv. India, Spec. Publ, Calcutta* **19** 144.

GSI 2002 Geothermal energy resources of India; *Geol. Surv. India, Spec. Publ. Calcutta* **69** 12–29.

Gunnell Y and Fleitout L 1998 Shoulder uplift of the Western Ghats passive margin, India: A denudational model; *Earth Surf. Process. Landf.* **23** 391–404.

Gupta H K, Arora K, Rao N P, Roy S, Tiwari V M, Patro P K, Satyanarayana H V S, Shashidhar D, Mahato C R, Srinivas K N S S S, Srihari M, Satyavani N, Srinu Y, Gopinadh D, Raza H, Jana M, Akkiraju V V, Goswami D, Vyas D, Dubey C P, Raju D Ch V, Borah L, Raju K, Reddy K C, Babu N, Bansal B K and Nayak S 2017 Investigations of continued reservoir triggered seismicity at Koyna, India; *Geol. Soc. London Spec. Publ.* **445** 151–188.

Hansen P 1992 Analysis of discrete ill-posed problems by means of the L-curve; *SIAM Rev.* **34** 561–580.

Harinarayana T, Abdul Azeez K K, Murthy D N, Veeraswamy K, Eknath Rao S P, Manoj C and Naganjaneyulu K 2006 Exploration of geothermal structure in Puga geothermal field, Ladakh Himalayas, India by magnetotelluric studies; *J. Appl. Geophys.* **58** 280–295.

Harinarayana T, Abdul Azeez K K, Naganjaneyulu K, Manoj C, Veeraswamy K, Murthy D N and Eknath Rao S P 2004 Magnetotelluric studies in Puga valley geothermal field, NW Himalaya, Jammu and Kashmir, India; *J. Volcanol. Geotherm. Res.* **138** 405–424.

Jones A G 2012 Distortion of magnetotelluric data: Its identification and removal; In: *The magnetotelluric method: Theory and practice* (eds) Chave A D and Jones A G, Cambridge University Press, New York, pp. 219–302.

Jones A G, Chave A D, Egbert G, Auld D and Bahr K 1989 A comparison of techniques for magnetotelluric response function estimation; *J. Geophys. Res.* **94** 14,201–14,213.

Jones A G and Jodicke H 1984 Magnetotelluric transfer function estimation improvement by a coherence-based rejection technique; In: *SEG technical program expanded abstracts*, SEG, pp. 51–55.

Kaila K L, Murthy P R K, Rao V K and Kharetchko G E 1981 Crustal structure from deep seismic sounding along the Koyna II (Kelsi–Loni) profile in the Deccan trap area, India; *Tectonophys.* **73** 365–384.

Kailasam L N, Murthy B G K and Chayanulu A Y S R 1972 Regional gravity studies of the Deccan trap areas of peninsular India; *Curr. Sci.* **41** 403–407.

Kale V S 2010 The Western Ghat: The great escarpment of India; In: *Geomorphological landscapes of the world* (ed.) Mignon P, Springer, Dordrecht, pp. 257–264.

Krieger L and Peacock J R 2014 MTpy: A python toolbox for magnetotelluric; *Comput. Geosci.* **72** 167–175.

Kumar D, Thiagarajan S and Rai S N 2011 Deciphering geothermal resources in Deccan trap region using electrical

resistivity tomography technique; *J. Geol. Soc. India* **78** 541–548.

Low U, Absar A, Duraiswami R and Singh A 2020 Geophysical exploration of Tural–Rajwadi group of hot springs, west coast geothermal province, Maharashtra, India and its implications; *Geothermics* **88** 101874.

McNeice G W and Jones A G 2001 Multisite, multifrequency tensor decomposition of magnetotelluric data; *Geophysics* **66** 158–173.

Minissale A, Vaselli O, Chandrasekharam D, Magro G, Tassi F and Casiglia A 2000 Origin and evolution of 'intracratonic' thermal fluids from central-western peninsular India; *Earth Planet Sci. Lett.* **181** 377–394.

Mohan K, Pavan Kumar G, Chaudhary P, Choudhary V K, Nagar M, Khuswaha D, Patel P, Gandhi D and Rastogi B K 2017 Magnetotelluric investigations to identify geothermal source zone near Chabsar hot water spring site, Ahmedabad, Gujarat, northwest India; *Geothermics* **65** 198–209.

Mohan G, Surve G and Tiwari P K 2007 Seismic evidences of faulting beneath the Panvel flexure; *Curr. Sci.* **93** 991–996.

Monterio A J, Duraiswami R A, Pujari S J, Absar A, Low U and Karmalkar N R 2019 Petrophysical variations within the basaltic lava flows from Tural-Rajawadi hot springs, western India and their bearing on the viability of low-enthalpy geothermal systems; *IOP Conf. Ser. Earth Environ. Sci.* **249**, https://doi.org/10.1088/1755-1315/249/1/012004.

Muir-Wood R and King G C P 1993 Hydrological signatures of earthquake strain; *J. Geophys. Res.* **98** 22,035–22,068.

Mukherjee S, Misra A A, Calvès G and Nemčok M 2017 Tectonics of the Deccan large igneous province: An introduction; In: *Tectonics of the Deccan large igneous province* (eds) Mukherjee S, Misra A A, Calvès G and Nemčok M, *Geol. Soc., London* **445** 1–9.

Negi J G, Agrawal P K, Singh A P and Pandey O P 1992 Bombay gravity high and eruption of Deccan flood basalts (India) from a shallow secondary plume; *Tectonophys.* **206(3)** 341–350, https://doi.org/10.1016/0040-1951(92)90385-J.

Nover G 2005 Electrical properties of crustal and mantle rocks – A review of laboratory measurements and their explanation; *Surv. Geophys.* **26** 593–651.

Owen H G 1976 Continental displacement and expansion of the Earth during Mesozoic and Cenozoic; *Phil. Trans. Soc. London* **281** 223–291.

Patro P K 2017 Magnetotelluric studies for hydrocarbon and geothermal resources: Examples from the Asian region; *Surv. Geophys.* **38** 1005–1041.

Pitale U L, Dubey R, Saxena R K, Prasad J M, Muthu-Raman K, Thussu J L and Sharma S C 1986 Review of geothermal studies of west coast hot spring belt, Maharashtra; *Rec. Geol. Surv. India* **115** 97–136.

Praveen Kumar K and Mohan G 2014 Crustal velocity structure beneath Saurashtra, NW India, through waveform modelling: Implications for magmatic underplating; *J. Asian Earth Sci.* **79** 173–181.

Radhakrishna T, Mohamed A R, Venkateshwarlu M and Soumya G S 2019 Mechanism of rift fank uplift and escarpment formation evidenced by Western Ghats, India; *Sci. Rep.* **9** 1–7.

RadhaKrishna M, Verma R K and Purushotham A K 2002 Lithospheric structure below the eastern Arabian Sea and adjoining west coast of India based on integrated analysis of gravity and seismic data; *Mar. Geophys. Res.* **23** 25–42.

Raval U 1993 The Regional Tectonothermal Setting of Killari (Latur) Area; In: *Proceedings of the 30th annual convention and seminar of IGU*, Hyderabad, 21–23 December 1993, pp. 169–180.

Raval U 1995 Seismicity of the Koyna region and regional tectonomagmatism of the western margin (India); *Pure Appl. Geophys.* **145** 175–192.

Raval U and Veeraswamy K 2003 Modification of geological and geophysical regimes due to interaction of mantle plume with Indian lithosphere; *J. Virtual Explorer* **12** 117–143.

Ray R, Shukla A D, Sheth H C, Ray J S, Duraiswami R A, Vanderkluysen L, Rautel C S and Mallik J 2008 Highly heterogeneous Precambrian basement under the central Deccan traps, India: Direct evidence from xenoliths in dykes; *Gondwana Res.* **13** 375–385.

Reddy D V, Nagabhushanam P and Ramesh G 2013 Turnover time of Tural and Rajwadi hot spring waters, Maharashtra, India; *Curr. Sci.* **104** 1419–1424.

Rodi W and Mackie R L 2001 Nonlinear conjugate gradients algorithm for 2-D magnetotelluric inversion; *Geophysics* **66** 174–187.

Sandiford M and Powell R 1986 Deep crustal metamorphism during continental extension: Modern and ancient examples; *Earth Planet. Sci. Lett.* **79** 151–158.

Sarolkar P B 2005 Geochemical characters of hot springs of west coast, Maharashtra state, India; In: *Proceedings world geothermal congress*, Antalaya, Turkey, pp. 24–29.

Sen G 2001 Generation of Deccan trap magmas; *Proc. Indian Acad. Sci. (Earth Planet. Sci.)* **110** 409–431.

Sheth H C 1998 A reappraisal of the coastal Panvel flexure, Deccan traps, as a listric-fault controlled reverse drag structure; *Tectonophys.* **294** 143–149.

Simpson F and Bahr K 2005 *Practical magnetotellurics*; Cambridge University Press, Cambridge.

Spichak V and Manzella A 2009 Electromagnetic sounding of geothermal zones; *J. Appl. Geophys.* **68** 459–478.

Storey M, Mahoney J J, Saunders A D, Duncan R A, Kelley S P and Coffin M F 1995 Timing of hotspot-related volcanism and the breakup of Madagascar and India; *Science* **267** 852–855.

Tripathi A, Shalivahan S S, Bage A K, Singh S and Yadav P K 2019 Audio-magnetotelluric investigation of Bakreswar geothermal province, eastern India; *J. Earth Syst. Sci.* **128** 1–10.

Trupti G, Singh H K and Chandrasekharam D 2016 Major and trace element concentrations in the geothermal springs along the west coast of Maharashtra, India; *Arab. J. Geosci.* **9** 1–15.

Watts A B and Cox K G 1989 The Deccan traps: An interpretation in terms of progressive lithospheric Cexure in response to a migrating load; *Earth Planet Sci. Lett.* **93** 85–97.

Zhang L, Hao T, Xiao Q, Wang J, Zhou L, Qi M, Cui X and Cai N 2015 Magnetotelluric investigation of the geothermal anomaly in Hailin, Mudanjiang, northeastern China; *J. Appl. Geophys.* **118** 47–65.